


Short-term toll-like receptor 9 inhibition leads to left ventricular wall thinning after myocardial infarction

Max Lenz^{1,2}, Attila Kiss^{2,3}, Patrick Haider^{1,2}, Manuel Salzmann¹, Mira Brekalo¹, Konstantin A. Krychtiuk^{1,2}, Ouafa Hamza³, Kurt Huber⁴, Christian Hengstenberg¹, Bruno K. Podesser³, Johann Wojta^{2,5}, Philipp J. Hohensinner^{2,3*}  and Walter S. Speidl^{1,2}

¹Department of Internal Medicine II, Division of Cardiology, Medical University of Vienna, Vienna, Austria; ²Ludwig Boltzmann Institute for Cardiovascular Research, Vienna, Austria; ³Center for Biomedical Research, Medical University of Vienna, Vienna, Austria; ⁴3rd Medical Department for Cardiology and Emergency Medicine, Faculty of Medicine, Wilhelminenhospital and Sigmund Freud University, Vienna, Austria; and ⁵Core Facility Imaging, Medical University of Vienna, Vienna, Austria

Abstract

Aims Ischaemia–reperfusion injury (IRI) following myocardial infarction remains a challenging topic in acute cardiac care and consecutively arising heart failure represents a severe long-term consequence. The extent of neutrophil infiltration and neutrophil-mediated cellular damage are thought to be aggravating factors enhancing primary tissue injury. Toll-like receptor 9 was found to be involved in neutrophil activation as well as chemotaxis and may represent a target in modulating IRI, aspects we aimed to illuminate by pharmacological inhibition of the receptor.

Methods and results Forty-nine male adult Sprague–Dawley rats were used. IRI was induced by occlusion of the left coronary artery and subsequent snare removal after 30 min. Oligonucleotide (ODN) 2088, a toll-like receptor 9 (TLR9) antagonist, control-ODN, or DNase, were administered at the time of reperfusion and over 24 h via a mini-osmotic pump. The hearts were harvested 24 h or 4 weeks after left coronary artery occlusion and immunohistochemical staining was performed. Echocardiography was done after 1 and 4 weeks to determine ventricular function. Inhibition of TLR9 by ODN 2088 led to left ventricular wall thinning ($P = 0.003$) in association with drastically enhanced neutrophil infiltration ($P = 0.005$) and increased markers of tissue damage. Additionally, an up-regulation of the chemotactic receptor CXCR2 ($P = 0.046$) was found after TLR9 inhibition. No such effects were observed in control-ODN or DNase-treated animals. We did not observe changes in monocyte content or subset distribution, hinting towards neutrophils as the primary mediators of the exerted tissue injury.

Conclusions Our data indicate a TLR9-dependent, negative regulation of neutrophil infiltration. Blockage of TLR9 appears to prevent the down-regulation of CXCR2, followed by an uncontrolled migration of neutrophils towards the area of infarction and the exertion of disproportional tissue injury resulting in potential aneurysm formation. In comparison with previous studies conducted in TLR^{−/−} mice, we deliberately chose a transient pharmacological inhibition of TLR9 to highlight effects occurring in the first 24 h following IRI.

Keywords CXCR2; Infarction; Ischaemia–reperfusion; Neutrophils; TLR9

Received: 12 December 2022; Revised: 7 April 2023; Accepted: 2 May 2023

*Correspondence to: Philipp Hohensinner, Center for Biomedical Research, Medical University of Vienna, Währingergürtel 18-20, 1090 Vienna, Austria.

Email: philipp.hohensinner@meduniwien.ac.at

Introduction

Cardiovascular diseases remain the most common cause of death within the western world. According to the American Heart Association, an estimate of one million coronary events occurred during the year 2019 in the United States.¹ Comparable data were presented in the Cardiovascular Disease

Statistics 2019 published by the European Society of Cardiology (ESC).² Although advances in medical therapy and improved reperfusion strategies have led to decreased mortality rates within the last decades, complications include ventricular aneurysm formation, potentially resulting in ventricular free-wall rupture, ventricular septal defects, and acute mitral regurgitation due to papillary muscle rupture lead to

a worsened outcome.³ Although reperfusion is crucial for myocardial salvage and the prevention of tissue-related complications, it bears the risk of further damaging the afflicted area.

The innate immune system is responsible for initiating the primary response following ischaemia and reperfusion (IR). Neutrophils are reported to significantly contribute to the sustained inflammatory response and overall severity of IR injury (IRI).⁴ A key factor in regulating chemotaxis and mounting an inflammatory response in neutrophils is the activation of toll-like receptors (TLRs) via danger-associated molecular patterns or pathogen-associated molecular patterns (PAMPs).⁵ With TLR9 being the main receptor involved in the detection of unmethylated extracellular DNA, blockage of pathogen-associated molecular patterns activation was proposed as a possible targeting strategy in IRI.⁶ In experimental infarction models, TLR9 knockout mice exhibited a significantly higher rate of mechanical complications, particularly ventricular free wall rupture paired with a decrease in survival.^{7,8} In contrast, short-term inhibition of TLR9 attenuated IRI after 60 min of reperfusion in an ex vivo model.⁹ In addition, TLR9 inhibition protected from cerebral IRI in a stroke model.¹⁰ As TLR9 recognizes unmethylated CpG oligonucleotides (ODNs), stimulation by synthetic ODNs was reported. Replacement of a few bases in the sequence results in an ODN without activatory properties. One of these inhibitory ODNs is ODN 2088, which exerts competitive inhibition by binding to the TLR9 receptor.¹¹ The aim of our study was to identify if TLR9 short-term inhibition through ODN 2088 would result in similar effects as long-term TLR9 knockout.

Methods

Rat model of myocardial ischaemia–reperfusion and drug treatment

Forty-nine male Sprague–Dawley rats (10–12 weeks old, 260–400 g body weight, Charles River, Massachusetts, USA) were anaesthetized by intraperitoneal injection of a mixture of xylazine (4 mg/kg; Bayer, Leverkusen, Germany) and ketamine (100 mg/kg; Dr E. Gräub AG, Bern, Switzerland). Animals were intubated and ventilated (rodent ventilator: air 9 mL/kg body weight, 75–85 strokes/min) and kept at 37.5–38.5°C using a rectal temperature probe and a temperature mat. IRI was induced as described previously.¹² The TLR9 inhibitor ODN 2088 (InvivoGen, California, USA) was administered at the onset of reperfusion via the femoral vein in a bolus of 400 µg. Simultaneously, a mini-osmotic pump (Alzet, mini-osmotic pump, model 2001D, California, USA) was implanted to dispense the compound at a rate of 66.667 µg/h (1600 µg over 24 h) for a steady-state concentra-

tion above 0.1 µM for 24 h. Analgesia was initiated by intraperitoneal injection of Piritramide (0.1 mL/kg body weight) preoperatively. Additionally, piritramide was applied via the drinking water as a postoperative analgesic regimen (2 ampules of piritramide with 30 mL of glucose 5% in 250 mL water). The animals were sacrificed 24 h or 4 weeks after IR. Blood samples were taken from the caudal vena cava and stored in mini-serum and EDTA tubes (Greiner Bio-One, Kremsmünster, Austria). Of the 49 animals, 46 underwent induced IRI, whereas three animals received sham treatment (thoracotomy without IRI). Ten animals died during the operation or within the following 24 h (23.256%; four control-ODN, three DNase, and three ODN-2088 treated). No differences were found for group allocation and death during/after surgery ($P = 0.820$). In three animals, no clear myocardial infarction was inducible (6.697%, verified by immunohistochemistry staining). Rats suffering from premature death and those without infarction were excluded from further analyses. Experimental setup and group allocation are outlined in *Figure S1*. Echocardiography was performed at baseline, 1 week after IR, as well as prior to sacrifice, and left ventricular (LV) ejection fraction, LV end-systolic diameter, and LV end-diastolic diameter were recorded as described previously.¹² Housing and experimental conditions were in accordance with the latest guidelines on the ethical use of laboratory animals and the 3Rs. A constant light/dark cycle was established, and the animals were fed a conventional chow diet and water ad libitum with 22°C temperature and 50–60% humidity. The experimental protocol was approved by the ethics committee for laboratory animal experiments at the Medical University of Vienna and the Austrian Ministry of Science, Research and Education (BMBWF-66.009/0173-V/3b/2019). The use of male rats only in these experiments can be seen as a limitation, which represents a potential selection bias due to the lacking representation of female physiology.

Compound dosage and administration

The TLR9 inhibitor ODN 2088 (InvivoGen, California, USA) was purchased and administered at the onset of reperfusion. The manufacturer reports inhibition of CpG-mediated TLR9 activity in concentrations of 0.1–10 µM. Therefore, we aimed to keep the calculated steady-state concentration above 0.1 µM for 24 h. At the onset of reperfusion, a bolus of 400 µg ODN 2088 was administered intravenously. Simultaneously, the mini-osmotic pump dispensed the compound at a rate of 66.667 µg/h (1600 µg over 24 h). Given an average body weight of 330 g, 65% body water, molecular weight for ODN 2088 of 4874 g/mol, a high bioavailability via absorption by tissue, and a suspected biological half-life of 45 min: a steady-state concentration of 0.11 µM after 24 h was calculated.^{13,14} To test our hypothesis, control-ODN (negative

control for ODN 2088, InvivoGen, California, USA) was purchased and administered in the same way as ODN 2088 (a bolus of 400 µg and simultaneously 66.667 µg/h for 24 h via mini-osmotic pump). Ge et al. previously used 20 µg DNase-1 (per rat) to evaluate its therapeutic potential in a model of IR.¹⁵ Therefore, we decided to utilize 20 µg DNase-1 (DNase I, Merck, Darmstadt, Germany) as an initial bolus and 20 µg over 24 h. In sham-treated animals (thoracotomy without IRI), 400 µL physiological saline solution was injected as a bolus followed by the implantation of a mini-osmotic pump also filled with physiological saline solution.

Immunohistochemistry staining

Rat hearts were fixed in paraffin as published previously.¹² Sectioning (5 µm) of the left ventricle was performed after the appearance of the mitral valve and sections between 240 and 260 µm were used. Masson's trichrome staining (trichrome staining kit, Merck, Darmstadt, Germany), neutrophil content (anti-granulocytes antibody, Abcam, Cambridge, UK), monocyte content (mouse anti-rat CD68, Bio-Rad - former AbD Serotec, California, USA) myeloperoxidase- (MPO antibody, R&D systems, Minnesota, USA), CitH4- (anti-histone H4 (citrulline 3), Antibody, Millipore, Massachusetts, USA), CXCR2 (CXCR2 polyclonal antibody, Thermo Fisher Scientific, Massachusetts, USA), and p65 (NFκB p65 monoclonal antibody, Thermo Fisher Scientific, Massachusetts, USA) staining was performed and subsequently evaluated in five independent picture sections per animal. All sections were analysed using TissueFAXS (V4, TissueGnostics, Vienna, Austria) and ImageJ (V1.5) software. CellProfiler (V4.2.0) was used to determine the MFI of CXCR2 on neutrophils (defined via shape, DAPI, and MPO expression) and p65 translocation in MPO or CD68 positive cells (defined via shape, DAPI, MPO, and CD68 expression). All analyses were carried out by a blinded member of the study team.

Enzyme-linked immunosorbent assay

Enzyme-linked immunosorbent assay for GRO/CINC-1 (GRO/CINC-1 (rat) ELISA kit, Enzo Life Sciences, Lausen, Switzerland) and troponin T (rat cardiac troponin T ELISA kit, MyBioSource, California, USA) were used according to the manufacturer's instructions.

Flow cytometry and applied gating strategy

In brief, 50 µL of EDTA-anticoagulated whole blood was stained with saturating concentrations of the following antibodies: CD11b/c (PerCP-eFluor 710, Thermo Fisher Scientific, Massachusetts, USA), anti-granulocyte marker (FITC,

eBioscience, California, USA), and CD43 (Alexa Fluor 647, BioLegend, California, USA) following standard protocols on an Attune NXT (Thermo Fisher). The entire gating strategy is shown in *Figure S2*.

Statistics

Data are presented as mean ± SD. When analysing two conditions, the Mann–Whitney *U* test was used for nonparametric data (determined by the Kolmogorov–Smirnov test), whereas the Student's *t*-test was used for parametric data. Multiple comparison analysis was achieved by ANOVA, followed by Bonferroni correction. GraphPad Prism (V8.0, California, USA) and SPSS (V26, IBM Armonk, New York, USA) were used for the statistical analyses. Statistical significance was defined as $P < 0.05$ if not indicated otherwise.

Results

To understand the impact of short-term inhibition of TLR9 using ODN 2088, we performed a rat model with IR. ODN 2088 and respective control-ODN were administered at the start of reperfusion with a bolus injection and in parallel via implantation of an osmotic pump for continuous substance release over the next 24 h. The effect of this short-term inhibition on long-term outcomes was measured 4 weeks after IR. LV wall thickness was found dramatically reduced in ODN 2088-treated rats as compared with those receiving control-ODN (control-ODN; 2.089 mm ± 0.633 mm vs. ODN 2088; 0.888 mm ± 0.334 mm, *Figure 1A*, $P = 0.003$). Furthermore, ODN 2088-treated animals displayed a significantly reduced LV mass compared with control-ODN-treated animals (control-ODN; 100% ± 8.7% vs. ODN 2088; 82.2% ± 9.6%, *Figure 1B*, $P = 0.011$). When analysing collagen content using Masson trichrome staining, no tangible difference between the two depicted groups was found (control ODN; 8.3% ± 3.1% vs. ODN 2088; 11.2% ± 2.6%, *Figure 1C*, $P = 0.126$).

Short-term inhibition of TLR9 led to pronounced myocardial tissue damage during the healing phase. To understand whether ODN 2088 induced acute effects, we investigated troponin T (TnT) as a marker of muscle damage and histologically quantified the size of neutrophil infiltration within the LV. Circulating levels of troponin T were significantly increased in ODN 2088, and control-ODN animals compared with sham-treated rats and were higher in ODN 2088 than in control-ODN animals (*Figure 2A*, sham; 13.67 pg/mL ± 7.64 pg/mL, control-ODN; 43.10 pg/mL ± 20.01 pg/mL, ODN 2088; 73.56 ± 24.65). Moreover, ODN 2088-treated rats displayed significantly enlarged areas of neutrophil-infiltration 24 h after IR compared with control-ODN and sham-treated animals (*Figure 2B*, control-ODN;

Figure 1 Long-term effect of TLR9 inhibition. Four weeks after IR, ventricular wall thickness was found significantly decreased in ODN 2088-treated rats compared with control-ODN (A, $P = 0.003$). Moreover, ODN 2088-treated animals displayed a significantly reduced left ventricular mass (B, $P = 0.011$). No difference was found in analysing collagen content in ODN 2088-treated animals versus control-ODN (C, $P = 0.126$). Data are presented as mean \pm SD. P -values <0.05 were considered statistically significant. The scale bar indicates 1 mm. $**P < 0.01$, $*P < 0.05$.

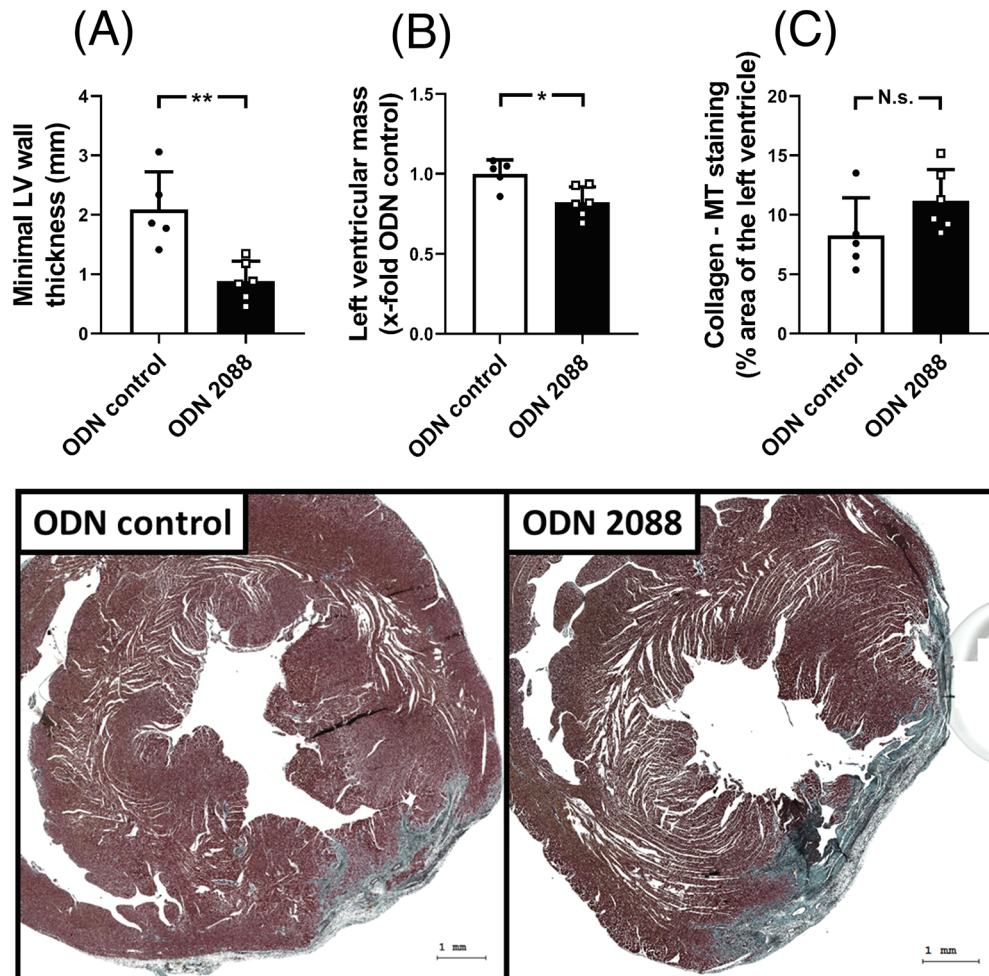
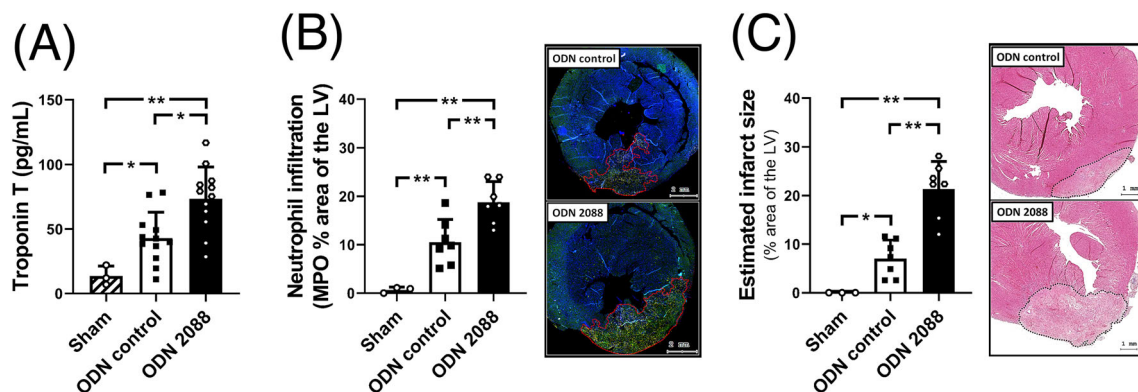


Figure 2 Short-term infarct parameters after TLR9 inhibition. Significant differences in circulating troponin T levels were detectable between sham-, control-ODN-, and ODN 2088-treated animals (A, $P = 0.029$, $P = 0.017$, $P = 0.007$, respectively). ODN 2088-treated rats displayed significantly enlarged areas of neutrophil infiltration after IR compared with control ODN (B, $P = 0.009$) as well as estimated infarct area (C, $P < 0.001$). Data are presented as mean \pm SD. P -values <0.05 were considered statistically significant. The scale bar indicates 2 or 1 mm. $**P < 0.01$, $*P < 0.05$.



10.56% \pm 4.71% vs. ODN 2088; 18.77% \pm 4.271%, $P = 0.005$). Furthermore, the estimated infarct area was also found to be increased (Figure 2C, control-ODN; 7.05% \pm 3.81% vs. ODN 2088; 21.35% \pm 5.69%, $P < 0.001$).

Myocardial infarction is followed by a robust inflammatory response and by infiltration of the infarcted area by innate immune cells.^{16,17} To understand if TLR9 inhibition changed the course of monocyte infiltration into the affected zone, we used immunohistochemical quantification of infiltrating monocytes into the infarcted area. Regarding monocyte content, no changes were found within the zone of infarction 24 h after IR (Figure 3A, sham; 184/mm² \pm 119/mm², control-ODN; 835/mm² \pm 281/mm² vs. ODN 2088; 723/mm² \pm 153/mm², $P = 0.371$). Furthermore, no statistically significant changes between ODN 2088 and control-ODN-treated animals were deducible at any time in circulating monocytes suggesting similar activation patterns for monocyte recruitment (Figure 3B). These findings were also supported when normalizing for baseline values (Figure 3C). As monocytes differentiate into specific subsets with different

functions, we also determined the distribution of monocyte subsets in the circulation after 24 h. Analysing monocyte subset distribution according to CD43 expression showed no statistically significant changes, indicating that TLR9 inhibition did not change the initial monocytic response nor distribution between subsets (Figure 3D).

Neutrophils are amongst the first responders to myocardial injury. Determining neutrophil content within the infarct area 24 h after IR, a pronounced increase was found in ODN 2088-treated animals compared with those receiving control-ODN (Figure 4A, sham; 37/mm² \pm 5/mm², control-ODN; 974/mm² \pm 479/mm² vs. ODN 2088; 1874/mm² \pm 352/mm², $P = 0.002$). In contrast, ODN 2088-treated animals displayed significantly decreased circulating neutrophil numbers 24 h after myocardial infarction and reperfusion determined by flow cytometry (Figure 4B, control-ODN; 3486/ μ L \pm 1396/ μ L vs. ODN 2088; 2262/ μ L \pm 841/ μ L, $P = 0.013$). When normalizing for neutrophil baseline values this finding prevailed (Figure 4C, control-ODN; 123.7% \pm 49.6% vs. ODN 2088; 75.9% \pm 28.2%, $P = 0.006$).

Figure 3 Monocytes after TLR9 inhibition. No changes in circulating monocyte content, infiltration of the zone of infarction, and CD43 expression were deducible at any point during the observational window (A–D). Data are presented as mean \pm SD. P -values < 0.05 were considered statistically significant. The scale bar indicates 20 μ m. ** $P < 0.01$, * $P < 0.05$.

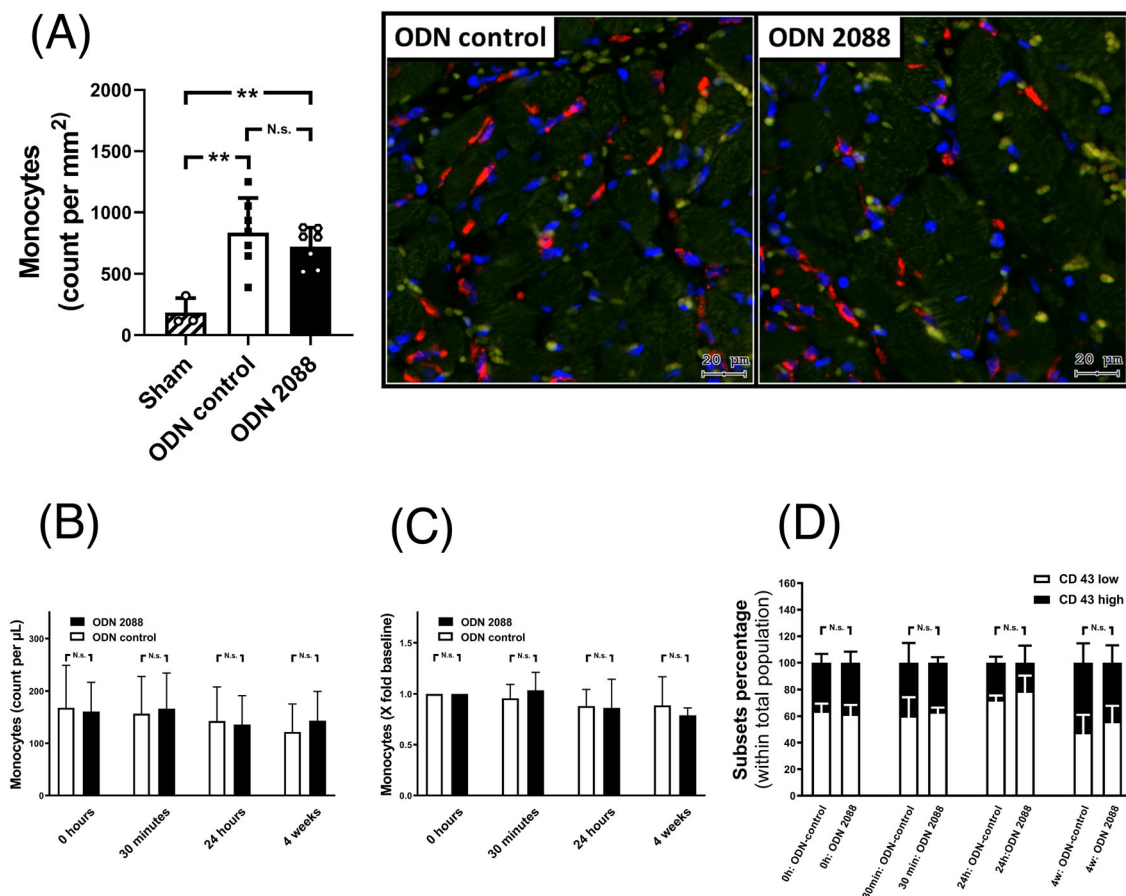
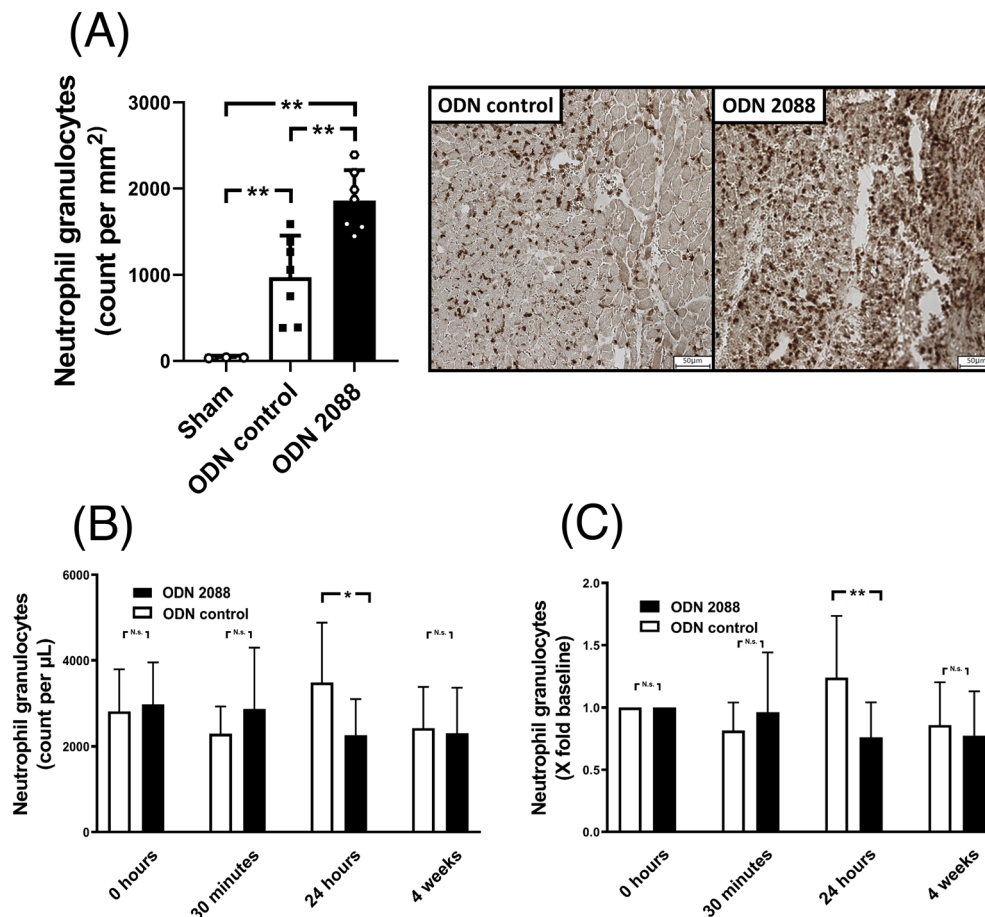


Figure 4 Neutrophils after TLR9-inhibition. Neutrophil content within the infarct area 24 h after IR, was found to increase in ODN 2088-treated animals compared with control ODN (A, $P = 0.002$). Using flow cytometry circulating neutrophils displayed decreased numbers at the same point in time (B, $P = 0.013$ and C, $P = 0.006$). Data are presented as mean \pm SD. P -values <0.05 were considered statistically significant. The scale bar indicates 50 μm . $**P < 0.01$, $*P < 0.05$.

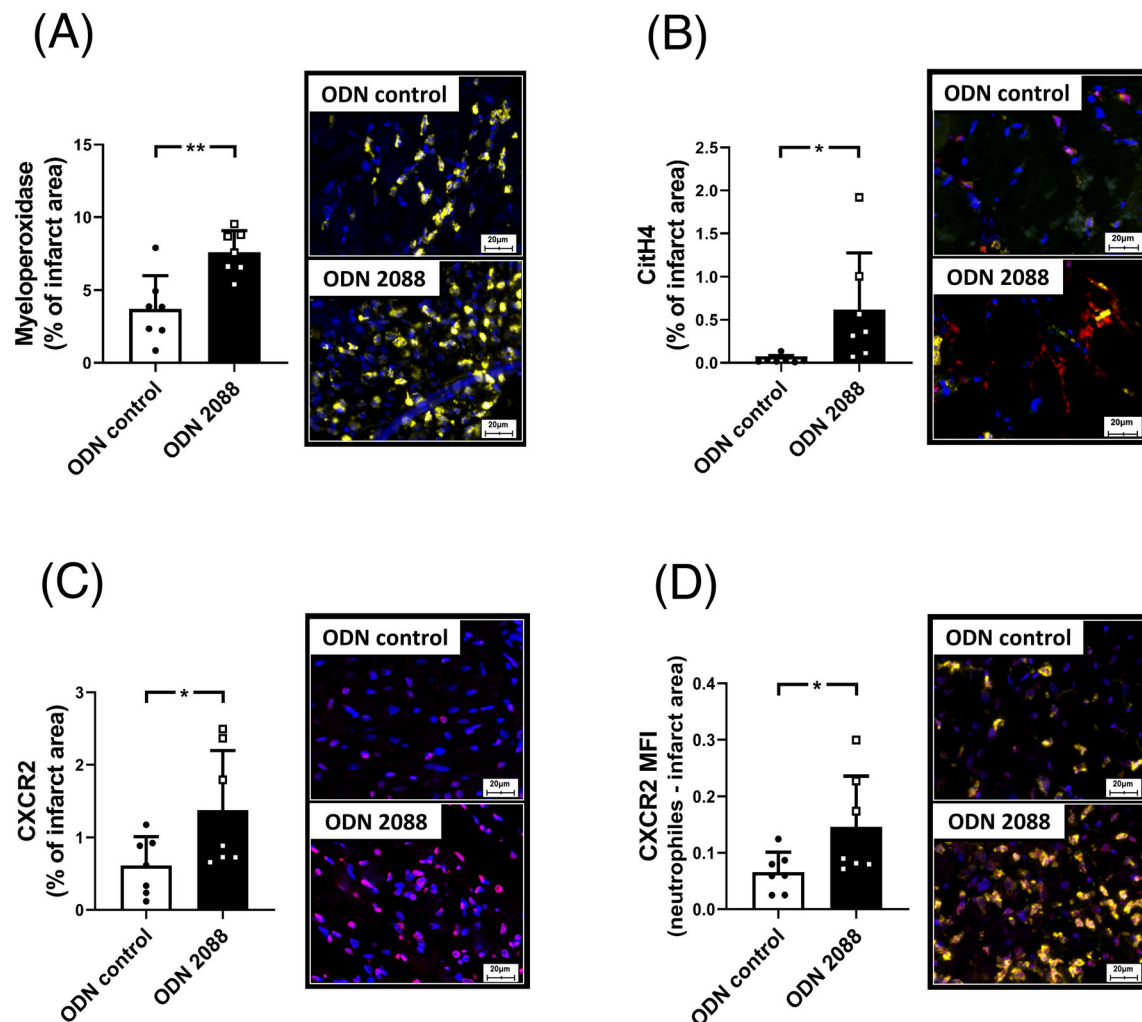


No changes in circulating neutrophil counts were detectable at baseline, 30 min, and 4 weeks thereafter, independent of normalization. To rule out potential thoracotomy-related changes in the numbers of circulating neutrophils and monocytes, sham surgery was performed on three rats. No procedure-induced changes were found by this approach (Figure S3A and S3B). Furthermore, NF κ B p65 nucleus translocation in CD68 positive cells was found increased in control ODN and DNase-treated animals compared with rats receiving sham treatment (Figure S5A). In neutrophils, ODN-control and ODN 2088 treatment resulted in similar p65 translocation with DNase-treated samples having no significant translocation of p65 in comparison with the sham group (Figure S5B).

To understand if the increased numbers are also reflected in changed activation profiles of neutrophils, we stained for the neutrophil activation marker MPO within the zone of infarction. We observed significantly more MPO staining in ODN 2088-treated animals compared with those treated with

control-ODN (Figure 5A, control-ODN; $3.71\% \pm 2.28\%$ vs. ODN 2088; $7.59\% \pm 1.49\%$, $P = 0.003$). Alongside, ODN 2088 treatment resulted in significantly higher citrullination of Histone 4 (citH4, Figure 5B, control-ODN; $0.037\% \pm 0.044\%$ vs. ODN 2088; $0.621\% \pm 0.653\%$, $P = 0.036$). Both MPO and citH4 are markers of highly activated neutrophils that are also capable to form neutrophil extracellular traps, a process where neutrophil DNA is released into the extracellular space.¹⁸ Previously, CXCR2-dependent recruitment of neutrophils to the infarcted area was reported to be crucial for tissue injury.¹⁹ CXCR2 positive cells were significantly increased in injured myocardium of animals receiving ODN (Figure 5C, control-ODN; $0.614\% \pm 0.398\%$ vs. ODN 2088; $1.380\% \pm 0.817\%$, $P = 0.045$). When analysing the mean fluorescence intensity (MFI) of CXCR2 on neutrophils, we found that rats treated with ODN 2088 displayed a significantly increased CXCR2-MFI as compared with animals treated with control-ODN (Figure 5D, control-ODN; 0.066 ± 0.035 vs. ODN 2088; 0.146 ± 0.090 , $P = 0.047$, arbitrary units). The cy-

Figure 5 Characterization of neutrophils after TLR9 inhibition. Twenty-four hours after IR, MPO-expression within the zone of infarction was found to increase in ODN 2088-treated animals compared with those treated with control-ODN (A, $P = 0.003$). Alongside, ODN 2088 treatment resulted in a significantly higher CitH4-expression (B, $P = 0.036$). Total CXCR2 expression (C, $P = 0.045$) and CXCR2-MFI on neutrophils were significantly increased after ODN 2088 treatment (D, $P = 0.047$). Data are presented as mean \pm SD. P -values < 0.05 were considered statistically significant. The scale bar indicates 20 μm . $**P < 0.01$, $*P < 0.05$.



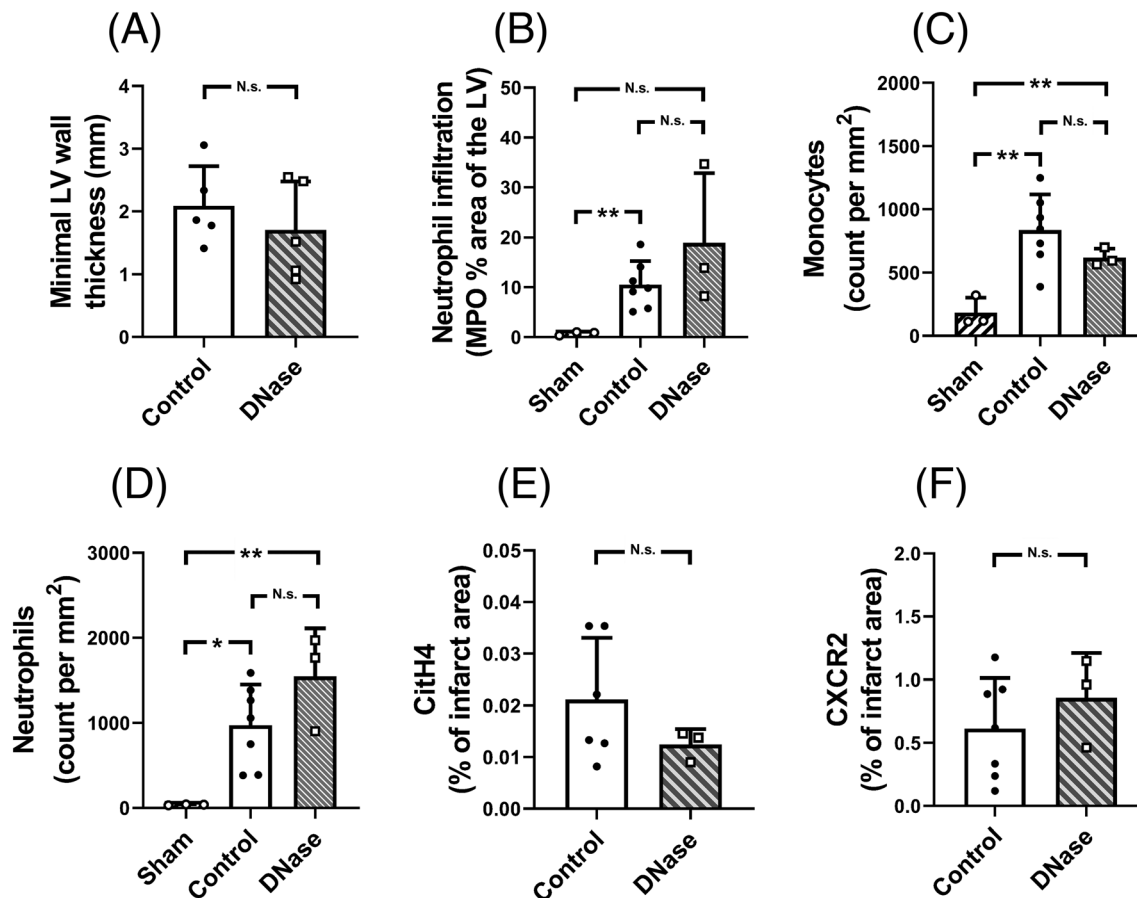
tokine for CXCR2 in rats is Gro/CINC-1, and no differences in serum levels were detectable in animals receiving ODN 2088 (Figure S3C, sham; 245.9 pg/mL \pm 129.4 pg/mL vs. control-ODN; 313.5 pg/mL \pm 239.5 pg/mL vs. ODN 2088; 241.2 pg/mL \pm 99.2 pg/mL, $P = 0.751$).

Echocardiography demonstrated a significant decrease of ejection fraction in animals treated with ODN 2088 and with control-ODN after one as well as 4 weeks, with no differences between the two groups at both time points (24 h: $P = 0.334$; 4 weeks: $P = 0.391$, data shown in Figure S4A). In contrast, to control treatment, animals treated with ODN 2088 showed a significant, rapid increase in end-diastolic diameter and end-systolic diameter 1 week after IR (Figure S4B and S4C). In contrast, after 4 weeks both treatment groups had significantly enlarged systolic and diastolic diameters by echocardi-

ography as compared with baseline with no significant differences between animals treated with ODN 2088 or control-ODN (Figure S4B and S4C).

ODN 2088 is a direct inhibitor of TLR9. To determine if similar observations are also true if one of the substrates for TLR9 is removed, we used DNase to degrade extracellular DNA. Four weeks after IR no changes in LV wall thickness were found comparing control-ODN and DNase-treated animals (Figure 6A, $P = 0.415$). Furthermore, no changes were found in area of neutrophil infiltration of the LV (Figure 6B, $P = 0.171$). When analysing the infarct area, we did not see differences in monocyte (Figure 6C, $P = 0.240$) or neutrophil infiltration (Figure 6D, $P = 0.137$). This similar infiltration pattern also suggests a similar activation status of neutrophils in the DNase group compared with control infarcts, which was

Figure 6 DNase treatment after IR. Four weeks after IR no changes in minimal ventricular wall thickness were found comparing control-ODN and DNase-treated animals (A, $P = 0.415$). Furthermore, no changes were found in MPO staining (B, $P = 0.171$), monocyte (C, $P = 0.240$) as well as neutrophil (D, $P = 0.137$) infiltration of the infarct zone, CitH4 (E, $P = 0.245$) and CXCR2 (D, $P = 0.391$) extent. Data are presented as mean \pm SD. P -values < 0.05 were considered statistically significant. $**P < 0.01$, $*P < 0.05$.



confirmed by similar content of CitH4 (Figure 6E, $P = 0.265$) or CXCR content (Figure 6F, $P = 0.391$).

Discussion

TLRs were found to play a pivotal role in the activation of the innate immune system. As DNA, including unmethylated CpG containing mitochondrial DNA, is present during tissue injury,²⁰ we were interested in the role of TLR9 activation following myocardial infarction. Our data indicate that early inhibition of TLR9-signalling results in worsened remodelling following ischaemia and subsequent reperfusion. Increased tissue damage and markedly elevated numbers of infiltrating neutrophils were found 24 h after IRI in ODN 2088-treated animals. These findings were underlined by concomitantly increased levels of troponin T. Previous studies on the topic produced mixed results. Utilizing a TLR9 agonist, Markowski *et al.* as well as Cao *et al.* reported an attenuation of IRI,

whereas Ohm *et al.* described no changes.^{21–23} However, Ohm *et al.* showed strong evidence of a reduced infiltration of granulocytes to the affected myocardium.²² Using a TLR9 antagonist, we demonstrated a worsened outcome with increased myocardial wall thinning.

Four weeks after IR, rats treated with ODN 2088 displayed pronounced LV wall thinning. Additionally, total LV mass was found noticeably decreased compared with animals treated with control-ODN. However, our findings report no changes in LV collagen content, hinting towards an aggravated early tissue injury as compared with impaired wound healing at later stages. Omiya *et al.* and Liu *et al.* reported a significantly reduced survival of TLR9^{−/−} mice used in a myocardial infarction model in which the animals were subjected to permanent ligation of the left coronary artery.^{7,8} The cause of death was found to be due to aneurysm formation and free wall rupture of the left ventricle. Although our methodical approach differs from the two reported ones, the effects appear similar. We deliberately restrained from using a genetic knockout model to highlight the implications of TLR9 block-

age within the first 24 h following IR and to understand possible treatment implications. Therefore, the aim of our experimental setup was to clarify the early involvement of neutrophils and monocytes in IRI in a transient compared with a constitutional model of TLR9 inhibition. Within the first 24 h, neutrophils are described as the predominant population at the site of infarction, followed by monocytes peaking between days 2 and 4.²⁴ Thus, our experimental setup was designed to focus on neutrophil recruitment and the associated tissue injury. In particular, later changes such as differences in macrophage polarization could be influenced by the permanently abolished TLR9 response in a knockout model. So the novelty of our experimental approach is an early and gated window of inhibition.

In contrast to monocytes, the numbers of circulating neutrophils were significantly reduced in ODN 2088-treated animals. In animal models, neutrophil depletion was reported to reduce infarct size and the extent of tissue injury.^{25,26} Accordingly, increased neutrophil counts after percutaneous coronary intervention for ST-elevation myocardial infarction were found to be associated with larger infarct sizes and worse cardiac function.²⁷ Neutrophil-derived tissue damage is exerted by various factors, including MPO induced formation of reactive oxygen intermediates or the emission of degranulation products such as proteases, collagenases, and lipoxygenases. Within the last decade, findings of an interrelation between myocardial reperfusion injury and the formation of neutrophil extracellular traps emerged.²⁸ Our findings underline these statements as MPO, and citrullinated histone H4 were found significantly increased in the infarcts of ODN 2088-treated rats 24 h after IR. Our proposed sequence of events constitutes the inhibition of TLR9, followed by drastically increased migration of neutrophils to the zone of infarction and results in short-term tissue injury and the depicted structural changes after 4 weeks. Interestingly, no changes in NF κ B p65 translocation were deducible for neutrophils with or without treatment when comparing to sham control. However, control ODN-treated animals displayed an increase in p65 translocation in CD68-positive cells compared with rats receiving sham treatment. No such effect was deducible comparing sham- and ODN 2088 treatment. These findings might hint towards priming of a less inflammatory phenotype in monocytes or resident macrophages.

In a sepsis model using TLR9^{-/-} mice, Trevelin et al. discovered an essential link between TLR9 activation and impaired chemotaxis in neutrophils where TLR9 deficiency prevented the down-regulation of the CXCR2 receptor, an important player in neutrophil chemotaxis.²⁹ Using ODN 2088, we observed increased expression of CXCR2 within the site of infarction 24 h after IR. Furthermore, no changes in GRO/CINC-1 alpha, a chemotactic substrate for CXCR2 in rats, were deducible at the same time. These findings indicate a similar chemotactic potential in treated and untreated animals. We suggest that inhibition of TLR9 leads to decreased

down-regulation of CXCR2, resulting in increased neutrophil infiltration to the infarct area. This finding was emphasized by the fact that not only total CXCR2 within the lesion but CXCR2 expression on neutrophils was found to be significantly elevated. With this finding, we aimed to close the loop from initial TLR9 inhibition to increased neutrophil migration and neutrophil-associated tissue injury, finally resulting in LV wall thinning and damage to the left ventricle. In addition to TLR9, ODN 2088 was reported to interact with TLR7 and TLR8. Both receptors were found to be inhibited by ODN 2088 resulting in a reduced inflammatory response.³⁰ Although both targets are reported to be involved in mounting immune responses, no clear link to chemotaxis, and in particular, CXCR2 expression was found in the literature. However, TLR7- and TLR8-mediated effects leading to adverse remodeling cannot be ruled out.

Finally, we tried to evaluate the differences in TLR9-blockage and substrate reduction. Therefore, key experiments done with ODN 2088 were repeated using DNase as unmethylated CpG sequences in DNA molecules are reported to activate TLR9.³¹ Furthermore, neutrophil extracellular traps (NETs) were implied to play a role in TLR9 activation.³² Ge et al. already demonstrated beneficial effects of DNase-induced reduction of NETs in IR.¹⁵ No differences in the primary readout of LV wall thinning were detectable 4 weeks after IR. Moreover, no significant changes were noticeable for immune cell infiltration, CItH4, and CXCR2 expression. These findings underline the differences in blockage of the TLR9 receptor versus substrate degradation. A possible explanation can be found in the different number of affected pathophysiological mechanisms. Whereas ODN 2088 administration 'only' blocks the TLR9 receptor, DNase application results in a reduction of substrate as well as in a depletion of structures directly damaging the afflicted area. Although our data clearly indicate a worse outcome in ODN 2088-treated animals, rats receiving DNase displayed a largely unaltered outcome. Despite this, a trend towards reduced LV mass ($P = 0.087$, data not shown) might be viewed as a warning sign for a potential therapeutic application of DNase.

Conclusions

Within the presented manuscript, we aimed to illuminate the consequences of TLR9 blockage in a rat model of IRI. Findings of pronounced LV wall thinning and aggravated short-term tissue damage were observed in animals treated with the TLR9 antagonist ODN 2088. Increased neutrophil infiltration towards the infarct zone and increased neutrophil-mediated tissue damage are believed to set these changes in motion. Combining our reports with previously published data on the chemotactic axis linking TLR9 activation to CXCR2 expres-

sion, the picture of a self-limiting physiological process appears plausible. Following this iteration, danger-associated molecular pattern-mediated activation of TLR9 results in pro-inflammatory stimulation of neutrophils and migration to the site of infarction, initially to clear debris and mount an immune response. However, continuous activation of TLR9 seems to down-regulate the expression of CXCR2, steadily reducing the chemotactic gradient to the lesion. Taking the exerted neutrophil-mediated tissue damage and decreasing numbers of neutrophils needed in later stages of tissue repair into account, such a regulatory feedback loop seems probable if not necessary. Pharmacological blockage of the TLR9 receptor appears to disrupt this process of down-regulating CXCR2. The following uncontrolled migration of neutrophils towards the area of infarction and the associated tissue damage are thought to constitute the previously discussed short as well as long-term effects. To our knowledge, we are the first to describe this potential sequence in a model of sterile inflammation (TLR9-dependent enhancement of neutrophil infiltration or TENI) with the main focus on the pharmacological inhibition of TLR9 within the first 24 h after IR. Taking our findings into account, pharmacological strategies involving TLR9 inhibition for the reduction of IRI seem to produce contrary results. In this regard, future projects in humans focusing on TLR inhibition during IRI should be appraised critically.

Funding

This project was funded by the Austrian Society of Cardiology and the Ludwig Boltzmann Institute for Cardiovascular Research.

Conflict of interest

The authors declare no conflict of interest.

Supporting information

Additional supporting information may be found online in the Supporting Information section at the end of the article.

Figure S1. Experimental overview.

Figure S2. Flow cytometry gating.

Figure S3. Sham and Gro/CINC-1.

Figure S4. Echo data.

Figure S5. NFkB p65 in neutrophils and CD68 positive cells.

References

1. Benjamin EJ, Muntner P, Alonso A, Bittencourt MS, Callaway CW, Carson AP, Chamberlain AM, Chang AR, Cheng S, Das SR, Dellings FN, Djousse L, Elkind MSV, Ferguson JF, Fornage M, Jordan LC, Khan SS, Kissela BM, Knutson KL, Kwan TW, Lackland DT, Lewis TT, Lichtman JH, Longenecker CT, Loop MS, Lutsey PL, Martin SS, Matsushita K, Moran AE, Mussolino ME, O'Flaherty M, Pandey A, Perak AM, Rosamond WD, Roth GA, Sampson UKA, Satou GM, Schroeder EB, Shah SH, Spartano NL, Stokes A, Tirschwell DL, Tsao CW, Turakhia MP, VanWagner LB, Wilkins JT, Wong SS, Virani SS, American Heart Association Council on Epidemiology and Prevention Statistics Committee and Stroke Statistics Subcommittee. Heart Disease and Stroke Statistics-2019 Update: A Report From the American Heart Association. *Circulation*. 2019;139:e56–e528. Erratum in: *Circulation*. 2020;141:e33.
2. Timmis A, Townsend N, Gale CP, Torbica A, Lettino M, Petersen SE, Mossialos EA, Maggioni AP, Kazakiewicz D, May HT, de Smedt D, Flather M, Zühlke L, Beltrame JF, Huculeci R, Tavazzi L, Hindricks G, Bax J, Casadei B, Achenbach S, Wright L, Vardas P, European Society of Cardiology, Mimosza L, Artan G, Aurel D, Chettibi M, Hammoudi N, Sisakian H, Pepoyan S, Metzler B, Siostrzonek P, Weidinger F, Jahangirov T, Aliyev F, Rustamova Y, Manak N, Mrochak A, Lancellotti P, Pasquet A, Claeys M, Kušljugić Z, Dizdarević Hudić L, Smajić E, Tokmakova MP, Gatzov PM, Milicic D, Bergovec M, Christou C, Moustra HH, Christodoulides T, Linhart A, Taborsky M, Hansen HS, Holmvang L, Kristensen SD, Abdelhamid M, Shokry K, Kampus P, Viigimaa M, Ryödi E, Niemelä M, Rissanen TT, le Heuzey JY, Gilard M, Aladashvili A, Gamkrelidze A, Kereselidze M, Zeiher A, Katus H, Bestehorn K, Tsioufis C, Goudevenos J, Csanádi Z, Becker D, Tóth K, Jóna Hrafnkelsdóttir Þ, Crowley J, Kearney P, Dalton B, Zahger D, Wolak A, Gabrielli D, Indolfi C, Urbini S, Imantayeva G, Berkinbayev S, Bajraktari G, Ahmeti A, Berisha G, Erkin M, Saamay A, Erglis A, Bajare I, Jegere S, Mohammed M, Sarkis A, Saadeh G, Zvirblyte R, Sakalyte G, Slapikas R, Ellafi K, el Ghamari F, Banu C, Beissel J, Felice T, Buttigieg SC, Xuereb RG, Popovici M, Boskovic A, Rabrenovic M, Ztot S, Abir-Khalil S, van Rossum AC, Mulder BJM, Elsendoorn MW, Srbinovska-Kostovska E, Kostov J, Marjan B, Steigen T, Mjølstad OC, Ponikowski P, Witkowski A, Jankowski P, Gil VM, Mimoso J, Baptista S, Vinereanu D, Chioncel O, Popescu BA, Shlyakhto E, Oganov R, Foscoli M, Zavatta M, Dikic AD, Beleslin B, Radovanovic MR, Hlivák P, Hatala R, Kaliská G, Kenda M, Fras Z, Anguita M, Cequier Á, Muñoz J, James S, Johansson B, Platonov P, Zellweger MJ, Pedrazzini GB, Carballo D, Shebli HE, Kabbani S, Abid L, Addad F, Bozkurt E, Kaykçioğlu M, Erol MK, Kovalenko V, Nesukay E, Wragg A, Ludman P, Ray S, Kurbanov R, Boateng D, Daval G, de Benito Rubio V, Sebastiao D, de Courtelary PT, Bardinet I. European Society of Cardiology: Cardiovascular Disease Statistics 2019. *Eur Heart J*. 2020; **41**: 12–85.
3. Bagai A, Dangas GD, Stone GW, Granger CB. Reperfusion strategies in acute coronary syndromes. *Circ Res*. 2014; **114**: 1918–1928.
4. Schofield ZV, Woodruff TM, Halai R, Wu MCL, Cooper MA. Neutrophils—a key component of ischemia-reperfusion injury. *Shock*. 2013; **40**: 463–470.
5. Vilahur G, Badimon L. Ischemia/reperfusion activates myocardial innate immune response: the key role of the

- toll-like receptor. *Front Physiol.* 2014; **5**: 496.
6. Shah M, Yellon DM, Davidson SM. The role of extracellular DNA and histones in Ischaemia-reperfusion injury of the myocardium. *Cardiovasc Drugs Ther.* 2020; **34**: 123–131.
 7. Liu FY, Fan D, Yang Z, Tang N, Guo Z, Ma SQ, Ma ZG, Wu HM, Deng W, Tang QZ. TLR9 is essential for HMGB1-mediated post-myocardial infarction tissue repair through affecting apoptosis, cardiac healing, and angiogenesis. *Cell Death Dis.* 2019; **10**: 480.
 8. Omiya S, Omori Y, Taneike M, Protti A, Yamaguchi O, Akira S, Shah AM, Nishida K, Otsu K. Toll-like receptor 9 prevents cardiac rupture after myocardial infarction in mice independently of inflammation. *Am J Physiol Heart Circ Physiol.* 2016; **311**: H1485–H1497.
 9. Kitazume-Taneike R, Taneike M, Omiya S, Misaka T, Nishida K, Yamaguchi O, Akira S, Shattock MJ, Sakata Y, Otsu K. Ablation of toll-like receptor 9 attenuates myocardial ischemia/reperfusion injury in mice. *Biochem Biophys Res Commun.* 2019; **515**: 442–447.
 10. Lu C, Ha T, Wang X, Liu L, Zhang X, Kimbrough EO, Sha Z, Guan M, Schweitzer J, Kalbfleisch J, Williams D, Li C. The TLR9 ligand, CpG-ODN, induces protection against cerebral ischemia/reperfusion injury via activation of PI3K/Akt signaling. *J Am Heart Assoc.* 2014; **3**: e000629.
 11. Stunz LL, Lenert P, Peckham D, Yi AK, Haxhinasto S, Chang M, Krieg A M, Ashman R F. Inhibitory oligonucleotides specifically block effects of stimulatory CpG oligonucleotides in B cells. *Eur J Immunol.* 2002; **32**: 1212–1222.
 12. Pilz PM, Hamza O, Gidlöf O, Gonçalves IF, Tretter EV, Trojanek S, Abraham D, Heber S, Haller PM, Podesser BK, Kiss A. Remote ischemic preconditioning attenuates adverse cardiac remodeling and preserves left ventricular function in a rat model of reperfused myocardial infarction. *Int J Cardiol.* 2019; **285**: 72–79.
 13. Cascella RRWM. *Steady State Concentration*. StatPearls; 2023.
 14. Palma E, Cho MJ. Improved systemic pharmacokinetics, biodistribution, and antitumor activity of CpG oligodeoxynucleotides complexed to endogenous antibodies in vivo. *J Control Release.* 2007; **120**: 95–103.
 15. Ge L, Zhou X, Ji WJ, Lu RY, Zhang Y, Zhang YD, Ma YQ, Zhao JH, Li YM. Neutrophil extracellular traps in ischemia-reperfusion injury-induced myocardial no-reflow: therapeutic potential of DNase-based reperfusion strategy. *Am J Physiol Heart Circ Physiol.* 2015; **308**: H500–H509.
 16. Hohensinner PJ, Niessner A, Huber K, Weyand CM, Wojta J. Inflammation and cardiac outcome. *Curr Opin Infect Dis.* 2011; **24**: 259–264.
 17. Mentkowski KI, Euscher LM, Patel A, Alevriadou BR, Lang JK. Monocyte recruitment and fate specification after myocardial infarction. *Am J Physiol Cell Physiol.* 2020; **319**: C797–C806.
 18. Hofbauer TM, Mangold A, Scherz T, Seidl V, Panzenböck A, Ondracek AS, Müller J, Schneider M, Binder T, Hell L, Lang IM. Neutrophil extracellular traps and fibrocytes in ST-segment elevation myocardial infarction. *Basic Res Cardiol.* 2019; **114**: 33.
 19. Schloss MJ, Horckmans M, Nitz K, Duchene J, Drechsler M, Bidzhekov K, Scheiermann C, Weber C, Soehnlein O, Steffens S. The time-of-day of myocardial infarction onset affects healing through oscillations in cardiac neutrophil recruitment. *EMBO Mol Med.* 2016; **8**: 937–948.
 20. Krychtiuk KA, Ruhittel S, Hohensinner PJ, Koller L, Kaun C, Lenz M, Bauer B, Wutzlhofer L, Draxler DF, Maurer G, Huber K, Wojta J, Heinz G, Niessner A, Speidl WS. Mitochondrial DNA and toll-like receptor-9 are associated with mortality in critically ill patients. *Crit Care Med.* 2015; **43**: 2633–2641.
 21. Markowski P, Boehm O, Goelz L, Haesner AL, Ehrentauf H, Bauerfeld K, Tran N, Zacharowski K, Weisheit C, Langhoff P, Schwederski M, Hilbert T, Klaschik S, Hoefl A, Baumgarten G, Meyer R, Knuefermann P. Pre-conditioning with synthetic CpG-oligonucleotides attenuates myocardial ischemia/reperfusion injury via IL-10 up-regulation. *Basic Res Cardiol.* 2013; **108**: 376.
 22. Ohm IK, Gao E, Belland Olsen M, Alfsnes K, Bliksøen M, Øgaard J, Ranheim T, Nymo SH, Holmen YD, Aukrust P, Yndestad A, Vinje LE. Toll-like receptor 9-activation during onset of myocardial ischemia does not influence infarct extension. *PLoS ONE.* 2014; **9**: e104407.
 23. Cao Z, Ren D, Ha T, Liu L, Wang X, Kalbfleisch J, Gao X, Kao R, Williams D, Li C. CpG-ODN, the TLR9 agonist, attenuates myocardial ischemia/reperfusion injury: involving activation of PI3K/Akt signaling. *Biochim Biophys Acta.* 2013; **1832**: 96–104.
 24. Nahrendorf M, Pittet MJ, Swirski FK. Monocytes: protagonists of infarct inflammation and repair after myocardial infarction. *Circulation.* 2010; **121**: 2437–2445.
 25. Chia S, Nagurney JT, Brown DFM, Raffel OC, Bamberg F, Senatore F, Wackers FJT, Jang IK. Association of leukocyte and neutrophil counts with infarct size, left ventricular function and outcomes after percutaneous coronary intervention for ST-elevation myocardial infarction. *Am J Cardiol.* 2009; **103**: 333–337.
 26. Jolly SR, Kane WJ, Hook BG, Abrams GD, Kunkel SL, Lucchesi BR. Reduction of myocardial infarct size by neutrophil depletion: effect of duration of occlusion. *Am Heart J.* 1986; **112**: 682–690.
 27. Jordan JE, Zhao ZQ, Vinten-Johansen J. The role of neutrophils in myocardial ischemia-reperfusion injury. *Cardiovasc Res.* 1999; **43**: 860–878.
 28. Savchenko AS, Borisoff JI, Martinod K, de Meyer SF, Gallant M, Erpenbeck L, Brill A, Wang Y, Wagner DD. VWF-mediated leukocyte recruitment with chromatin decondensation by PAD4 increases myocardial ischemia/reperfusion injury in mice. *Blood.* 2014; **123**: 141–148.
 29. Trevelin SC, Alves-Filho JC, Sônego F, Turato W, Nascimento DC, Souto FO, Cunha TM, Gazzinelli RT, Cunha FQ. Toll-like receptor 9 activation in neutrophils impairs chemotaxis and reduces sepsis outcome. *Crit Care Med.* 2012; **40**: 2631–2637.
 30. Jurk M, Kritzler A, Schulte B, Tluk S, Schetter C, Krieg A M, Vollmer J. Modulating responsiveness of human TLR7 and 8 to small molecule ligands with T-rich phosphorothiate oligodeoxynucleotides. *Eur J Immunol.* 2006; **36**: 1815–1826.
 31. Martinez-Campos C, Burguete-Garcia AI, Madrid-Marina V. Role of TLR9 in oncogenic virus-produced cancer. *Viral Immunol.* 2017; **30**: 98–105.
 32. Bruschi M, Moroni G, Sinico RA, Franceschini F, Fredi M, Vaglio A, Cavagna L, Petretto A, Pratesi F, Migliorini P, Manfredi A, Ramirez GA, Esposito P, Negrini S, Trezzi B, Emmi G, Santoro D, Scolari F, Volpi S, Mosca M, Tincani A, Candiano G, Prunotto M, Verrina E, Angeletti A, Ravelli A, Ghiggeri GM. Neutrophil extracellular traps in the autoimmunity context. *Front Med (Lausanne).* 2021; **8**: 614829.